Journal of the American Heart Association

ORIGINAL RESEARCH

CircALMS1 Alleviates Pulmonary Microvascular Endothelial Cell Dysfunction in Pulmonary Hypertension

Xiaoyi Hu, MD*; Yuanyuan Sun, MD*; Shang Wang, MD*; Hui Zhao, MD; Yaqin Wei, MS; Jiaqi Fu, MS; Yuxia Huang ⓘD, MD; Wenhui Wu, MD; Jinling Li, MS; Jinming Liu, MD; Sugang Gong ⓘD, MD; Qinhua Zhao, MD; Lan Wang, MD; Rong Jiang ⓘD, MD; Xiao Song ⓘD, PhD; Ping Yuan ⓘD, MD

BACKGROUND: Circular RNAs can serve as regulators influencing the development of pulmonary hypertension (PH). However, their function in pulmonary vascular intimal injury remains undefined. Thus, we aimed to identify specifically expressed circular RNAs in pulmonary microvascular endothelial cells (PMECs) under hypoxia and PH.

METHODS AND RESULTS: Deep RNA sequencing and quantitative real-time polymerase chain reaction revealed that circALMS1 (circular RNA Alstrom syndrome protein 1) was reduced in human PMECs under hypoxia ($P<0.0001$). Molecular biology and histopathology experiments were used to elucidate the roles of circALMS1 in regulating PMEC dysfunction among patients with PH. The circALMS1 expression was decreased in the plasma of patients with PH ($P=0.0315$). Patients with lower circALMS1 levels had higher risk of death ($P=0.0006$). Moreover, the circALMS1 overexpression of adeno-associated viruses improved right ventricular function and reduced pulmonary vascular remodeling in monocrotaline-PH and sugen/hypoxia-PH rats ($P<0.05$). Furthermore, circALMS1 overexpression promoted apoptosis and inhibited PMEC proliferation and migration under hypoxia by directly downregulating miR-17-3p ($P<0.05$). Dual luciferase assay confirmed the direct binding of circALMS1 to miR-17-3p and miR-17-3p binding to its target gene YT521-B homology domain-containing family protein 2 (YTHDF2) ($P<0.05$). The YTHDF2 levels were also downregulated in hypoxic PMECs ($P<0.01$). The small interfering RNA YTHDF2 reversed the effects of miR-17-3p inhibitors on PMEC proliferation, migration, and apoptosis. Finally, the results indicated that, although YTHDF2, as an N(6)-methyladenosine reader protein, contributes to the degradation of many circular RNAs, it could not regulate the circALMS1 levels in PMECs ($P=0.9721$).

CONCLUSIONS: Our study sheds new light on circALMS1-regulated dysfunction of PMECs by the miR-17-3p/YTHDF2 pathway under hypoxia and provides insights into the underlying pathogenesis of PH.

Key Words: circALMS1 ■ hypoxia ■ pulmonary hypertension ■ pulmonary microvascular endothelial cells ■ pulmonary vascular remodeling

Endothelial cells (ECs) form the selectively permeable monolayer on the luminal surface of blood vessels. They maintain vascular homeostasis through their anticoagulant and anti-inflammatory effects by regulating vascular tone and permeability.[1,2] EC dysfunction is a major feature of various vascular diseases, such as pulmonary hypertension (PH). PH is a complex multifactorial disease and is characterized by functional and structural alterations of the pulmonary circulation that cause a marked increase in pulmonary vascular resistance, ultimately leading to right-sided heart failure and death.[2–4] As a key initial

CLINICAL PERSPECTIVE

What Is New?

- A novel circAMLS1 (circular RNA Alstrom syndrome protein 1) was downregulated in pulmonary hypertension.
- CircALMS1 regulates the proliferation, migration, and apoptosis of pulmonary microvascular endothelial cells by regulating the miR-17-3p/YTHDF2 (YT521-B homology domain-containing family protein 2) axis.

What Are the Clinical Implications?

- Our results showed that circALMS1 may be a promising diagnostic and prognostic indicator for patients with pulmonary hypertension.

Nonstandard Abbreviations and Acronyms

AAV	adeno-associated virus
circALMS1	circRNA Alstrom syndrome protein 1
circGSAP	circular γ-secretase activating protein
circRNA	circular RNA
EC	endothelial cell
FISH	fluorescence in situ hybridization
IPAH	idiopathic pulmonary arterial hypertension
m6A	N(6)-methyladenosine
meRIP	methylated RNA immunoprecipitation
NC	normal control
PH	pulmonary hypertension
PMEC	pulmonary microvascular endothelial cell
qRT-PCR	quantitative reverse transcription polymerase chain reaction
RVSP	right ventricular systolic pressure
SuHx	sugen/hypoxia
YTHDF2	YT521-B homology domain-containing family protein 2

event of PH, EC dysfunction is triggered by hypoxia, inflammation, and other processes.[5,6] Under adverse conditions, apoptosis-resistant pulmonary microvascular ECs (PMECs) with a greater proliferative capacity progressively emerge and lead to proliferative plexiform lesions.[5–7] Despite substantial improvements over the past decades in PH diagnosis and treatment, patients with PH still have a poor prognosis.[8] Therefore, novel

therapeutic targets for PMECs are urgently needed in the treatment of PH.

Circular RNAs (circRNAs) play a pivotal role in various disease processes. circRNAs are a kind of single-stranded, covalently closed noncoding RNAs without 5′ end caps or 3′ end poly (A) tails.[9–11] Accumulating evidence indicated that circRNAs can potentially serve as biomarkers in the diagnosis, prognosis, and treatment of vascular diseases.[12–14] Recently, many studies have focused on the mechanism of circRNAs impacting PH development; most of these studies reported that circRNAs can affect the function of pulmonary arterial smooth muscle cells in PH.[15–17] PMECs are the first barrier for maintaining normal blood circulation, and its dysfunction also influences the pathophysiological processes of PH. The underlying mechanism of circRNAs in regulating the PMEC phenotype remains far from comprehension and needs further investigation.

Here, we aimed to identify specifically expressed circRNAs in PMECs that are involved in the context of hypoxia and PH. Using whole transcriptome sequencing, circALMS1 (circRNA Alstrom syndrome protein 1) was picked out and validated, which showed decreased expression in PMECs under hypoxia. We further investigated the role of circALMS1 in the proliferation, migration, and apoptosis of PMECs, and it may serve as a potential indicator in the diagnosis and prognosis of PH. Our results provided insights into the underlying pathogenesis of PH.

METHODS

The data supporting this study's findings are available from the corresponding author upon reasonable request.

Clinical Samples

Human plasma samples of 69 patients with PH and 69 healthy participants were obtained from Shanghai Pulmonary Hospital from January 2016 to October 2022. These 69 patients with PH include 33 patients with idiopathic pulmonary arterial hypertension (IPAH) and 36 patients with PH with chronic obstructive pulmonary disease. Lung tissues were obtained from a patient with PH undergoing lung transplantation at Shanghai Pulmonary Hospital. The baseline characteristics of the patient with PH undergoing lung transplantation are shown in Table S1. PH diagnosis was established according to the European Society of Cardiology and European Respiratory Society Guidelines.[18] The present study was approved and supervised by the Ethics Committee of Shanghai Pulmonary Hospital (No. K20-150Y). Written informed consent was obtained from all study participants.

Construction of the circALMS1 Adeno-Associated Virus and Intratracheal Injection

The circALMS1 sequence was cloned into the pHBAAV-CMV-circ-EF1-ZsGreen vector, which was then packaged into adeno-associated viruses (AAVs) from Hanheng Company (Hanheng Biotechnology Co., Ltd., Shanghai, China). Rats were anesthetized using isoflurane and given 200 μL of pHBAAV6-CMV-circALMS1-EF1-ZsGreen ($1.1×10^{12}$ vg/mL) via intratracheal injection to induce circALMS1 overexpression. Control rats were treated with the normal control (NC) vectors.

Animal Studies

Male Sprague-Dawley rats (180–220 g) were provided by Tongji University, Shanghai, China. The experiments were conducted in accordance with the *Guide for the Care and Use of Laboratory Animals*. The Ethics Committee of the Laboratory Animal Center of Tongji University School of Medicine approved the protocol, with the ethics number TJ-HB-LAC-2023-33.

For monocrotaline-PH animal models, 36 rats were randomly divided into the following 4 groups: control, monocrotaline, monocrotaline plus intratracheal injection of AAV NC (monocrotaline-AAV-NC), and monocrotaline
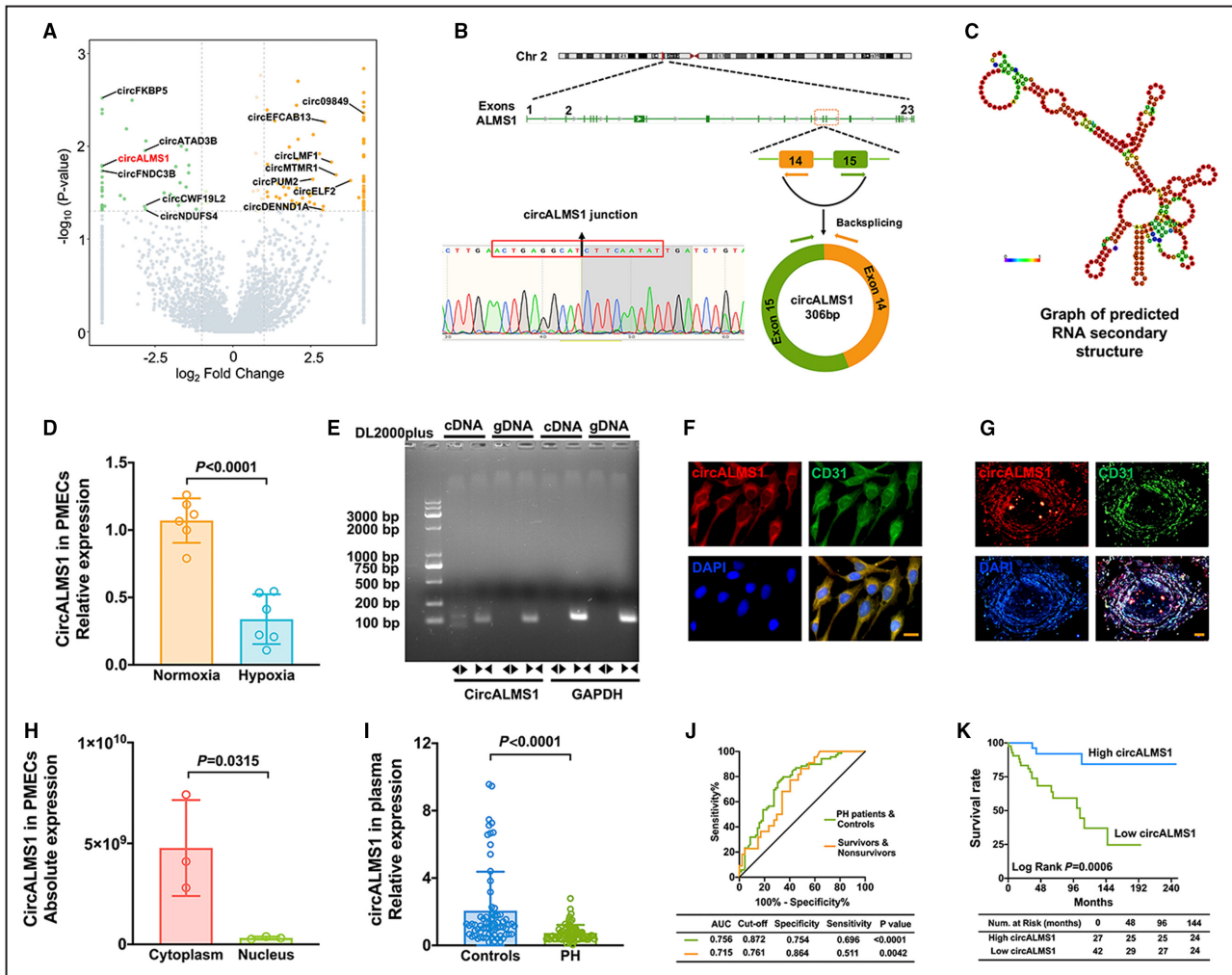
Figure 1. **CircALMS1 is downregulated in hypoxic PMECs and the plasma of patients with PH.**
A, Volcano map analysis of circRNAs in hypoxic PMECs. **B**, Genomic loci of ALMS1 gene. The backsplice junction of circALMS1 was identified by Sanger sequencing. **C**, Prediction of stem-loop structures of circALMS1 by using RNAFOLD WebServer (http://rna.tbi.univie.ac.at/). **D**, qRT-PCR analysis of circALMS1 expression in hypoxic PMECs (n=6). **E**, PCR analysis for circALMS1 and its linear isoform ALMS1 in cDNA and genomic DNA. **F**, FISH was used to determine the distribution of circALMS1 in PMECs. **G**, FISH was used to determine the distribution of circALMS1 in patients with PH. **H**, Absolute levels of circALMS1 in the nuclear and cytoplasmic fractions of PMECs (n=3). **I**, circALMS1 expression in plasma of PH patients (n=69). **J**, ROC curves of circALMS1 in patients with PH and survivors and nonsurvivors with PH. **K**, Kaplan–Meier survival analysis for death stratified by the cutoff values of circALMS1 in PH. All data are presented as the mean±SD. Scale bar, 100 μm. CircALMS1 indicates circular RNA Alstrom syndrome protein 1; FISH, fluorescence in situ hybridization; PH, pulmonary hypertension; PMECs, pulmonary microvascular endothelial cells; qRT-PCR, quantitative reverse transcription polymerase chain reaction; and ROC, receiver operating characteristic.
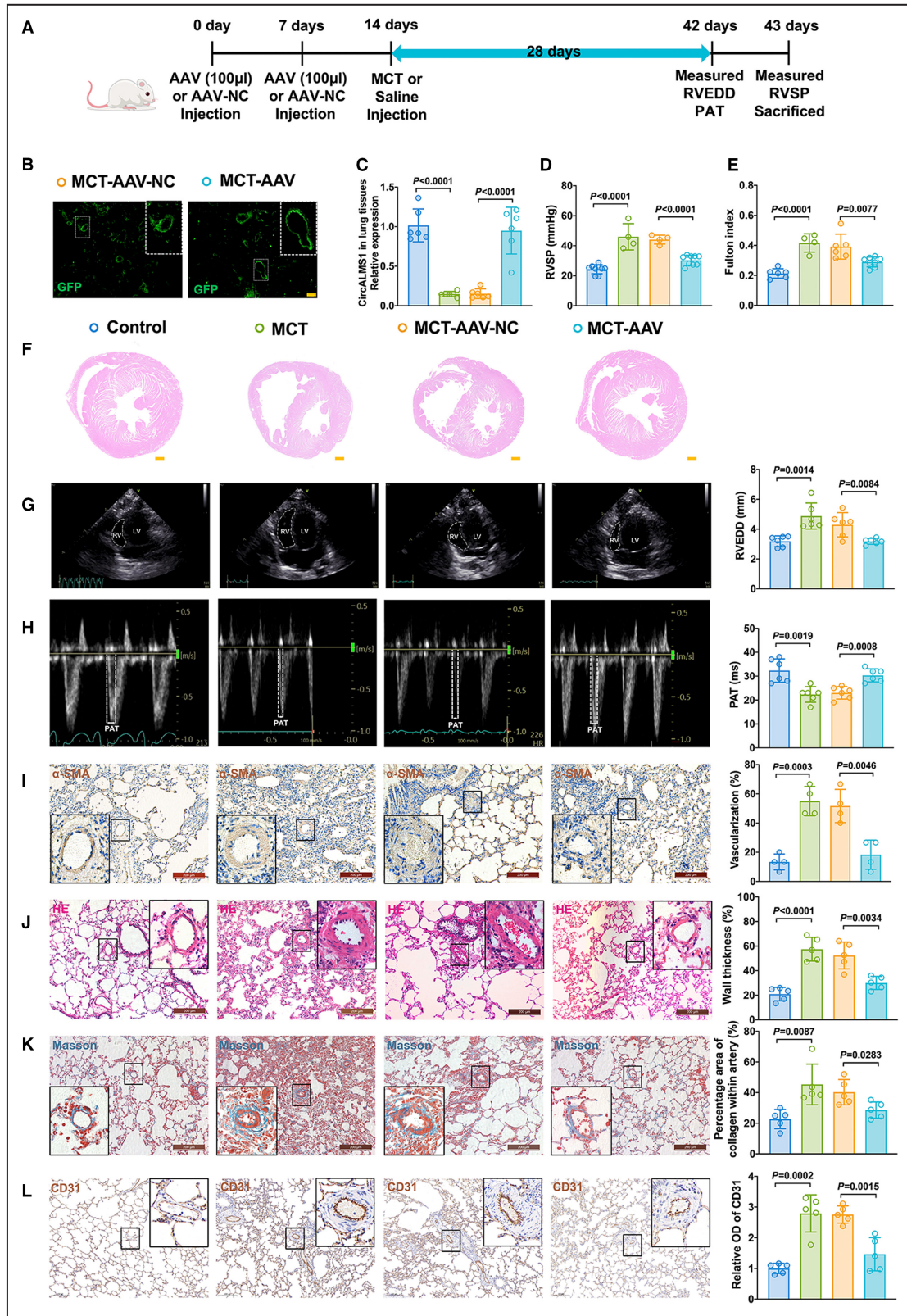
plus intratracheal injection of AAV (monocrotaline-AAV). For the monocrotaline-AAV-NC and monocrotaline-AAV groups, rats were intratracheally injected with AAV NC or AAV 14 days before the monocrotaline treatment.

Then, the monocrotaline, monocrotaline-AAV-NC, and monocrotaline-AAV groups were given a single intraperitoneal injection of monocrotaline (60 mg/kg). Control rats were given the equivalent volume of normal saline.

Figure 2. Effects of circALMS1 on the progression of monocrotaline-PH rats.
A, Flow chart of the animal experiment. **B** and **C**, GFP signals in the pulmonary arterial intima and the expression of circALMS1 in the lung tissues of animal models (n=6). **D** and **E**, RHC analysis of RVSP and the Fulton index in the control, monocrotaline, monocrotaline-AAV-NC, and monocrotaline-AAV groups. **F**, Histology of the cross-sectioned heart at the mid-right ventricular plane from rats. **G** and **H**, Echocardiography analysis of the RVEDD and PAT in the control, monocrotaline, monocrotaline-AAV-NC, and monocrotaline-AAV groups (n=6). **I** through **L**, Morphological analysis of the pulmonary artery was performed using α-smooth muscle actin, hematoxylin and eosin, Masson staining, and CD31 (n=4 or 5). All data are presented as mean±SD. Scale bar, 100 μm (**B**); 500 μm (**F**). AAV indicates adeno-associated virus; circALMS1, circular RNA Alstrom syndrome protein 1; GFP, green fluorescent protein; HE, hematoxylin and eosin; MCT-PH, monocrotaline-induced pulmonary hypertension; PAT, pulmonary artery acceleration time; RHC, right heart catheterization; RVEDD, right ventricular end-diastolic diameter; and RVSP, right ventricular systolic pressure.

Rats were housed for another 4 weeks from the day of injection.

For sugen/hypoxia (SuHx)-PH animal models, 32 rats were randomly divided into the 4 groups: control, SuHx, SuHx-AAV-NC, and SuHx-AAV. For the SuHx-AAV-NC and SuHx-AAV groups, rats were intratracheally injected with AAV NC or AAV 14 days before the SuHx treatment. Then, the SuHx, SuHx-AAV-NC, and SuHx-AAV groups were given a single intraperitoneal injection of sugen 5416 (20 mg/kg), followed by housing in a normobaric hypoxic chamber with 10% O_2 for 3 weeks and transferred into a normobaric normoxic chamber for another 2 weeks. Control rats were given the equivalent volume of normal saline and housed in a normobaric hypoxic chamber for 5 weeks.

Right Ventricular Systolic Pressure and Fulton Index Measurement

After the rats were anesthetized with 150 mg/kg sodium pentobarbital via intraperitoneal injection, the right external jugular vein was exposed and a polyethylene catheter with an internal diameter of 0.9 mm was inserted into the right ventricle. The catheter was connected to a pressure recorder (BL-420F) to record the right ventricular systolic pressure (RVSP). Then, rats were euthanatized, and tissues, including the heart and lung tissues, were collected for subsequent experiments. The Fulton index was calculated as the ratio of right ventricular weight to the left ventricle plus septum weight. Additionally, the left lung tissues were immersed in 4% paraformaldehyde, whereas the right lung tissues and hearts were stored at −80 °C.

Echocardiography

Transthoracic echocardiography was performed with a Vevo 2100 ultrasound machine (Visual Sonics, Toronto, Ontario, Canada). For anesthesia, rats were placed on a heated pad with continuous isoflurane inhalation (1%–2.5%). The fur on the chest was removed with a chemical hair remover. Transthoracic echocardiography was performed to measure the right ventricular end diastolic diameter and pulmonary artery acceleration time.

Histological Examination

After fixing with 4% paraformaldehyde for 48 hours, the left lung tissues were used for histological examination. Hematoxylin and eosin staining (Solarbio, Beijing, China), immunohistochemistry staining of α-smooth muscle actin (ab124964, Abcam, Cambridge, MA), immunohistochemistry staining of CD31 (28083-1-AP; Proteintech, Rosemont, IL), and Masson trichrome staining were performed as per manufacturer's instructions as described previously.[19] These sections were microphotographed by light microscopy (DP73; Olympus Corporation, Tokyo, Japan).

Mammalian Cell Lines

All primary cell lines of human PMECs were purchased from Science Cell (BK-3000; Shanghai, China). Briefly, the primary PMECs were cultured in the endothelia cell medium (BK-1001, Shanghai, China) in a CO_2 (5%) atmosphere at 37 °C. For hypoxic culture, PMECs were exposed to CO_2 (5%)/O_2 (3%)/balanced by N_2.

Whole Transcriptome Sequencing

Human PMECs (n=3) were exposed to hypoxia (3% O_2) or normoxia for 48 hours. The whole transcriptome sequencing was performed using total RNA of PMECs under hypoxia and normoxia by using an Illumina sequencing platform (TruSeq Stranded Total RNA with Ribo-Zero Gold/ HiSeqTM 4000; Illumina, San Diego, CA). The sequencing procedure and data analyses were performed by OEbiotech (Shanghai, China). Differentially expressed genes were identified using DESeq software.

Plasmid, Small Interfering RNA, and Cell Transfection

The circALMS1 sequence was amplified and cloned into a circRNA overexpression vector pLC5-ciR (Geneseed, Guangzhou, China). The primers used for cloning are listed in Table S2. Three small interfering RNAs (siRNAs) targeting circALMS1 and YTHDF2 were designed and synthesized by GenePharma (Shanghai, China). The sequences of circALMS1 and YTHDF2 siRNAs are listed in Table S2. For circALMS1 overexpression and silencing and YTHDF2 silencing, PMECs
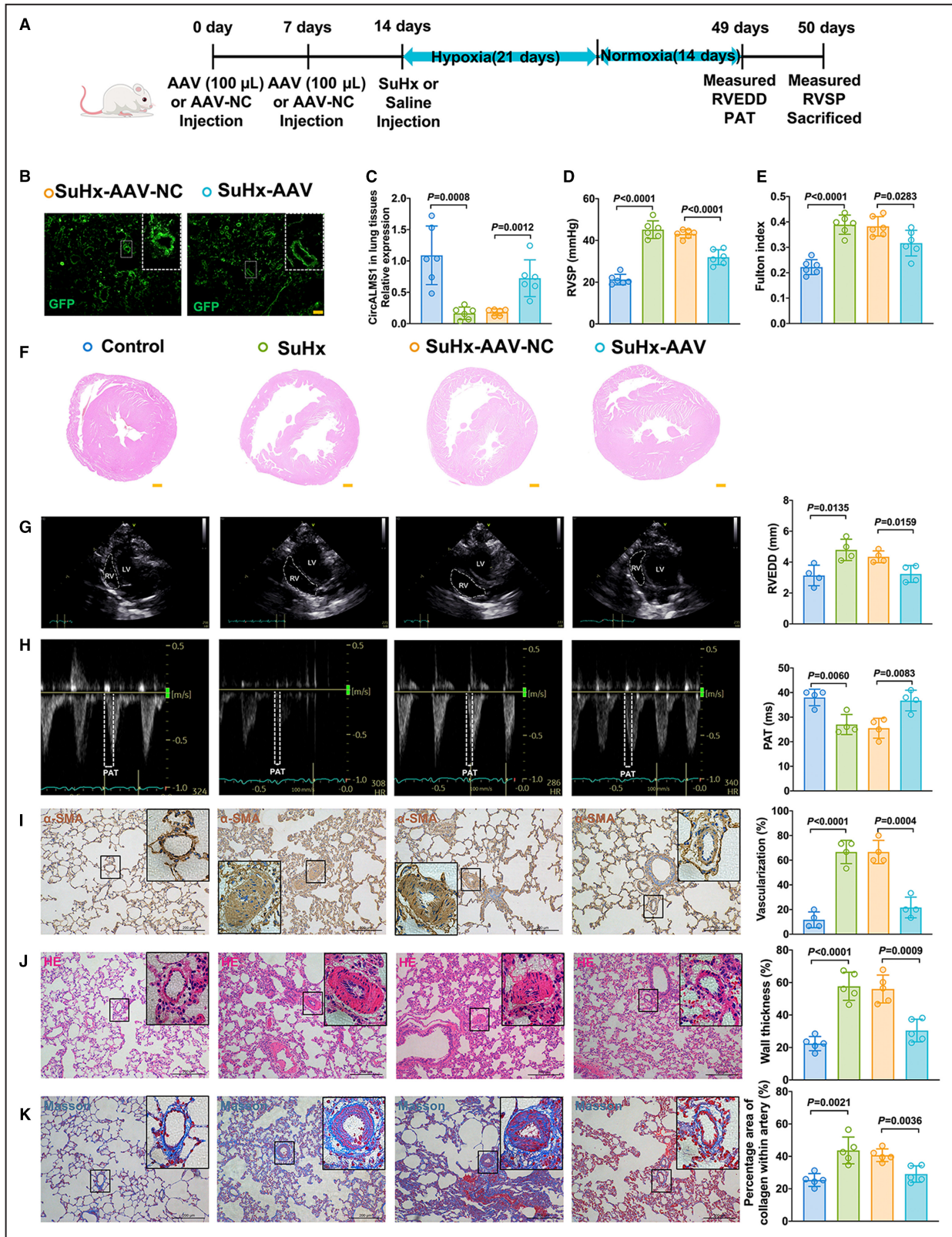
were transfected with 2 µg overexpression plasmid or 80 nmol/L siRNA by using Lipo2000 Transfection Reagent (Invitrogen, Waltham, MA).

For miR-17-3p overexpression and inhibition, PMECs were transfected with 40 nmol/L miR-17-3p mimics or 80 nmol/L miR-17-3p inhibitor (GenePharma, Shanghai,

Figure 3. Effects of circALMS1 on the progression of SuHx-PH rats.
A, Flow chart of the animal experiment. **B** and **C**, GFP signals in the pulmonary arterial intima and the expression of circALMS1 in the lung tissues of animal models (n=6). **D** and **E**, RHC analysis of RVSP and the Fulton index in the control, SuHx, SuHx-AAV-NC, and SuHx-AAV groups (n=6). **F**, Histology of the cross-sectioned heart at the mid-RV plane from rats. **G** and **H**, Echocardiography analysis of the RVEDD and PAT in the control, SuHx, SuHx-AAV-NC, and SuHx-AAV groups (n=4). **I** through **K**, Morphological analysis of the pulmonary artery was performed using α-smooth muscle actin, HE, and Masson staining (n=4 or 5). All data are presented as mean±SD. Scale bar, 100 μm (**B**); 500 μm (**F**). AAV indicates adeno-associated virus; circALMS1, circular RNA Alstrom syndrome protein 1; GFP, green fluorescent protein; HE, hematoxylin and eosin; PAT, pulmonary artery acceleration time; RHC, right heart catheterization; RVEDD, right ventricular end-diastolic diameter; RVSP, right ventricular systolic pressure; and SuHx-PH, sugen/hypoxia-induced pulmonary hypertension.

China) by using Lipo2000 Transfection Reagent (Invitrogen). The sequences are listed in Table S2. The control group was treated with equal concentrations of nontargeting mimic or inhibitor negative control sequences to control for nonspecific effects.

Cell Proliferation Assay

Altogether, 100 μL cells (2×10^4/mL) were seeded onto 96-well dishes and maintained at 37 °C for 4 hours. A Cell Counting Kit-8 (Dojindo, Japan) was used to measure cell proliferation at 0, 24, 48, and 72 hours. Briefly, 10 μL Cell Counting Kit-8 was added to each well and incubated at 37 °C for 2 hours. The absorbance value (optical density) was then measured at 450 nm filter using a microplate reader.

Wound Healing Assay

The Culture Insert-2 Well (Ibidi, Gräfelfing, Germany; Catalog No. 81176) was used for the wound healing assay. After adjusting the PMEC density of 1×10^6 cells/mL, 70-μL cells were seeded into each Culture Insert-2 Well. After an incubation for 24 hours, a starvation medium (ECM containing 1% FBS) was used to arrest cell growth. Then, the Culture Insert 2 Well was gently removed and the nonadherent cells were washed with PBS. A phase-contrast image was taken with an Olympus inverted microscope (IX51, Olympus). After 24 hours, the second image was captured. Relative migration was characterized as the percentage of wound area compared with the initial wound area.

Transwell Assay

In brief, 200 μL cells (10^5 cells/mL) that were resuspended with a free medium were added to the upper compartment of the migration chambers (BD Biosciences, San Jose, CA). The bottom chamber was filled with 500 μL cell culture ECM with 5% FBS as an attractant. After 24 hours, cells were fixed and stained with Crystal Violet Staining Solution (BL802A; Biosharp) and counted under microscopic observation.

Calcein-AM/Propidium Staining

Altogether, 500 μL PMECs were cultured on 24-well plates (4×10^4 cells/mL) for 24 hours. Then, the cells were

analyzed for fluorescence by calcein-AM/propidium (AM-PI) staining (Calcein-AM/PI Double Stain Kit; YEASEN Biotech Co., Shanghai, China). Experiments were conducted according to the manufacturer's instructions. For each sample, 5 μL (2 μmol/L) calcein-AM and 5 μL (2 μmol/L) PI were added to the cells and incubated for 30 minutes in an incubator (37 °C) in the dark. Then, the cells were analyzed using a fluorescence microscope.

Cell Apoptosis Assay

Annexin V, 633 Apoptosis Detection Kit (AD11, Dojindo) was used to measure the cell apoptosis rate according to the manufacturer's instructions. Briefly, 1.5 mL of PEMCs (2×10^5 cells/mL) were seeded onto a 6-well plate and incubated for 48 hours. After being harvested and washed with cold PBS twice, the cells were stained by 5 μL of annexin V and 5 μL of PI solution in in the dark for 15 minutes. Finally, the cells were detected using flow cytometry.

Dual Luciferase Activity Reporter System

To elucidate the circRNA–miRNA interaction, a circALMS1/YTHDF2 sequence containing the potential target sites for miR-17-3p was synthesized and cloned into the pGL3-promoter downstream of firefly luciferase (circAMLS1-WT/YTHDF2-WT). Mutant circALMS1/YTHHDF2 (circALMS1-MUT/YTHDF2-MUT) was also constructed with the mutation of the potential target sites. After cotransfection of the reporter vector and miR-17-3p mimics or negative control in 293T cells, the firefly luciferase activity was measured using a dual luciferase assay kit (Promega, Madison, WI) against that of Renilla luciferase. Each assay was repeated for 5 independent experiments. Primers and oligonucleotide sequence are listed in Table S2.

RNA Fluorescence In Situ Hybridization

After fixing with 4% paraformaldehyde for 15 minutes, cells were treated with 0.3% Triton X-100. Then, RNA hybridization buffer was added to cells for prehybrization at 55 °C for 2 hours. A fluorescently labeled junction probe was added to the cells and incubated at 37 °C overnight. Images were captured by confocal microscopy. The detection probe sequence is Table S2.

RNA Isolation, Reverse Transcription, and Quantitative Reverse Transcription Polymerase Chain Reaction

Total RNA samples were extracted from cultured PMECs and lung tissues using TRIZOL reagent (Invitrogen) according to the manufacturer's protocol. Cytoplasmic and nuclear RNAs were isolated using a PARIS™ kit (Thermo Fisher Scientific, Waltham, MA) according to the manufacturer's protocol. For each sample, 1 µg of total RNA was applied for cDNA conversion using the Superscript First-Strand cDNA Synthesis Kit (Invitrogen). Quantitative reverse transcription polymerase chain reaction (qRT-PCR) was carried out in a LightCycler 480 II qRT-PCR system (Roche, Germany) with SYBR Green I (Applied Biosystems, Waltham, MA). The cycle threshold was used to analyze the relative mRNA and miRNA levels using the $2^{-\Delta\Delta CT}$ method. The data were analyzed using the $2^{-\Delta\Delta CT}$ method. GAPDH or U6 mRNA was selected to normalize candidate gene expression. The key primers are listed in Table S2.

Genomic DNA Extraction

A genomic DNA isolation kit (Sangon Biotech, Shanghai, China) was used to extract the genomic DNA according to the manufacturer's instructions.

Protein Isolation and Western Analyses

Protein expression was analyzed using a standard Western blotting protocol.[20] Briefly, protein lysates were electrophoretically separated on SDS-PAGE and transferred to polyvinylidene fluoride membranes. After blocking in 5% milk for 1 hour, the membranes were bathed with β-actin monoclonal antibody (66009-1Ig, Proteintech; diluted 1:1000) and YTHDF2 polyclonal antibody (24744-1-AP, Proteintech; diluted 1:1000) overnight at 4 °C. The next day, the membranes were washed with Tris-buffered saline with 0.1% Tween 20 detergent and bathed with secondary antibodies (Proteintech; diluted 1:5000) for 1 hour.

M6A Methylated RNA Immunoprecipitation Assay

The N(6)-methyladenosine (m6A) methylated RNA immunoprecipitation (meRIP) assay was conducted by using a m6A meRIP Kit (BersinBio, Guangzhou, China; Catalog No. Bes5293-2). Briefly, total RNA was extracted from PMECs and fragmented into 300 nt using fragmentation buffer. Then, the samples were incubated with magnetic protein A/G conjugated 4 µg m^6A antibody or immunoglobulin G antibody. After extracting the RNA, enrichment of m^6A-containing circALMS1 segments was analyzed through qRT-PCR.

RNA Immunoprecipitation Assay

The RNA immunoprecipitation assay was conducted by using a Magna RIP Kit (17–700, Millipore, Burlington, MA). Briefly, PMECs from 5 dishes (10-cm cell culture dish) were harvested and washed with PBS, followed by lysing with RNA immunoprecipitation buffer. Then, the samples were incubated with magnetic protein A/G (Millipore, Catalog No.CS203178) conjugated YTHDF2 antibody (5 µg; Proteintech) and immunoglobulin G (Millipore, Catalog PP64B). After extracting the RNA, the circALMS1 level was analyzed by qRT-PCR.

Statistical Analysis

The data are presented as mean±SD. Two independent samples *t*-tests were carried out to compare the differences between 2 groups. One-way ANOVA and Tukey's multiple comparisons test were performed to compare the differences among ≥3 groups. Receiver operating characteristic (ROC) curve and the area under the ROC curve were determined, with the expression of circALMS1 treated as the test variable and the grouping based on the presence and absence of PH treated as the state variable, to explore the diagnostic efficacy of circALMS1 in PH. For the other ROC curve, the expression of circALMS1 was treated as the test variable and the grouping based on the survivor or nonsurvivor was treated as the state variable to explore the prognostic efficacy of circALMS1 in PH. The optimal cutoff was determined by the value that results in the maximum sum of sensitivity and specificity. Patients were divided into a low circALMS1 expression group and a high circALMS1 expression group on the basis of the cutoff value. The Kaplan–Meier method was then used to generate survival curves, and the log-rank test was used to compare the difference of the survival curve between different groups. Data management and analyses were performed with SPSS (IBM, Armonk, NY) and Prism 8.0 (GraphPad Software, La Jolla, CA). All tests were 2-tailed, and statistical significance was reported at $P<0.05$.

RESULTS

CircALMS1 Is Downregulated in Hypoxic PMECs and the Plasma of Patients With PH

To analyze the dysregulated circRNAs in hypoxic PMECs, high-throughput transcriptome sequencing was performed to identify the differentially expressed circRNAs. Our data showed 86 upregulated and 41 downregulated circRNAs in PMECs under hypoxia (|log2FC|>1 and $P<0.05$; Figure 1A). Particularly, low levels of circALMS1 were observed in PMECs under hypoxia, which was consistent with the sequencing
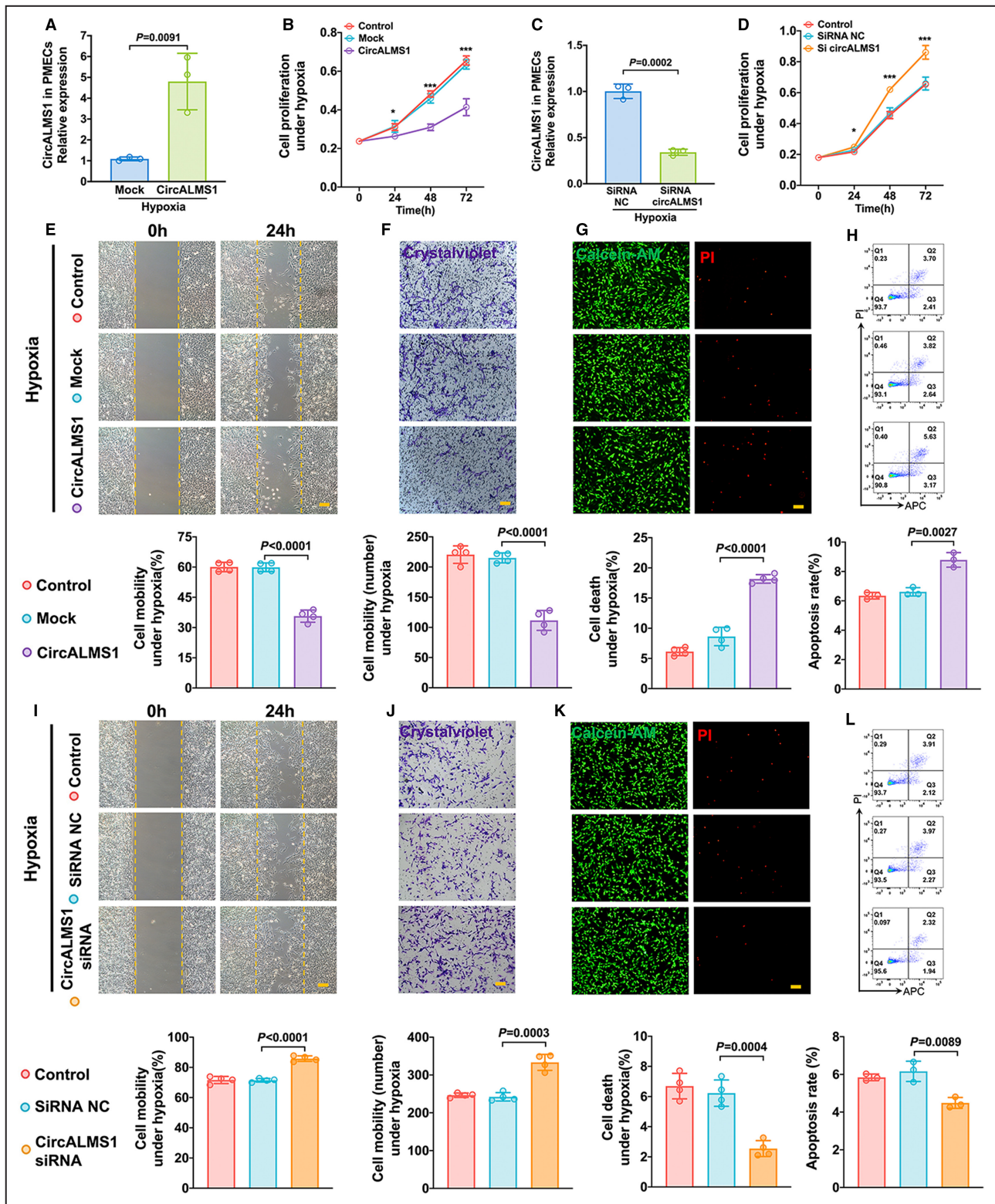
Figure 4. CircALMS1 suppresses proliferation and migration and promotes apoptosis of PMECs.
A, The overexpression efficiency of circALMS1 in hypoxic PMECs by qRT-PCR (n=3). **B** and **E** through **H**, Cell proliferation analysis, wound healing analysis, transwell analysis, AM-PI analysis, and apoptosis analysis of PMECs with overexpressing circALMS1 under hypoxia (n=5, 4, or 3). **C** The knockdown efficiency of circALMS1 in hypoxic PMECs by qRT-PCR (n=3). **D** and **I** through **L**, Cell proliferation analysis, wound healing analysis, transwell analysis, AM-PI analysis, and apoptosis analysis of PMECs with circALMS1 siRNA under hypoxia (n=5, 4, or 3). All data are presented as mean±SD. Scale bar, 100 μm. *P<0.05; **P<0.01; ***P<0.001. AM-PI indicates calcein-AM/propidium; CircALMS1, circular RNA Alstrom syndrome protein 1; PMECs, pulmonary microvascular endothelial cells; and qRT-PCR, quantitative reverse transcription polymerase chain reaction.

results (Figure 1D). Based on the transcriptome and Sanger sequencing results, circALMS1, with a total length of 306 bp, was generated from exons 14 and 15 of pre-mRNA ALMS1, which was located on human chromosome 2:73557220_73559142 (Figure 1B). The secondary structure of circALMS1 was predicted by RNAFOLD WebServer (http://rna.tbi.univie.ac.at/) (Figure 1C). Moreover, circALMS1 was amplified using divergent primers in cDNA, whereas no amplification was observed in the genomic DNA samples (Figure 1E).

A specific probe at the backsplice junction for fluorescence in situ hybridization (FISH) analysis was designed to determine the circALMS1 distribution. The results showed that circALMS1 was colocalized with the EC marker CD31 and was expressed in the ECs (Figure 1F and 1G). Additionally, absolute qRT-PCR analysis for nuclear and cytoplasmic circALMS1 was conducted, and the results showed that circALMS1 was predominantly expressed in the cytoplasm (Figure 1H).
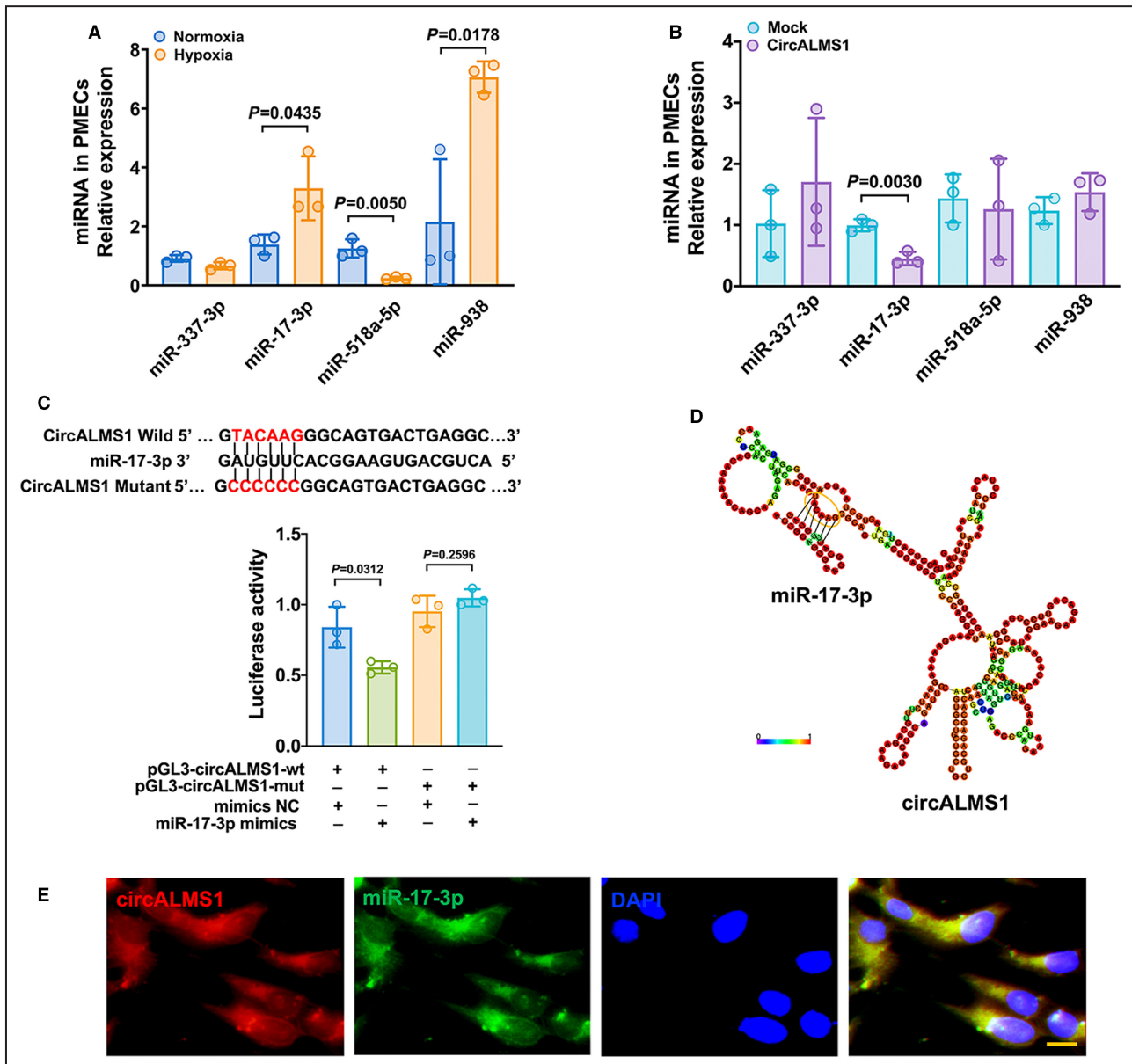
Figure 5.   CircALMS1 acts as an efficient miRNA sponge for miR-17-3p.
A and **B**, qRT-PCR was used to detect miRNA expression in hypoxic PMECs and circALMS1 overexpressed PMECs (n=3). **C**, Dual-luciferase assays were used to validate the interactions between circALMS1 and miR-17-3p (n=3). **D**, The predicted secondary structure for potienal binding sites between circALMS1 and miR-17-3p. **E**, FISH was used to observe the colocalization of circALMS1 and miR-17-3p in the cytoplasm of PMECs. All data are presented as mean±SD. Scale bar, 20 μm. CircALMS1 indicates circular RNA Alstrom syndrome protein 1; FISH, fluorescence in situ hybridization; miRNA, microRNA; PMECs, pulmonary microvascular endothelial cells; and qRT-PCR, quantitative reverse transcription polymerase chain reaction.
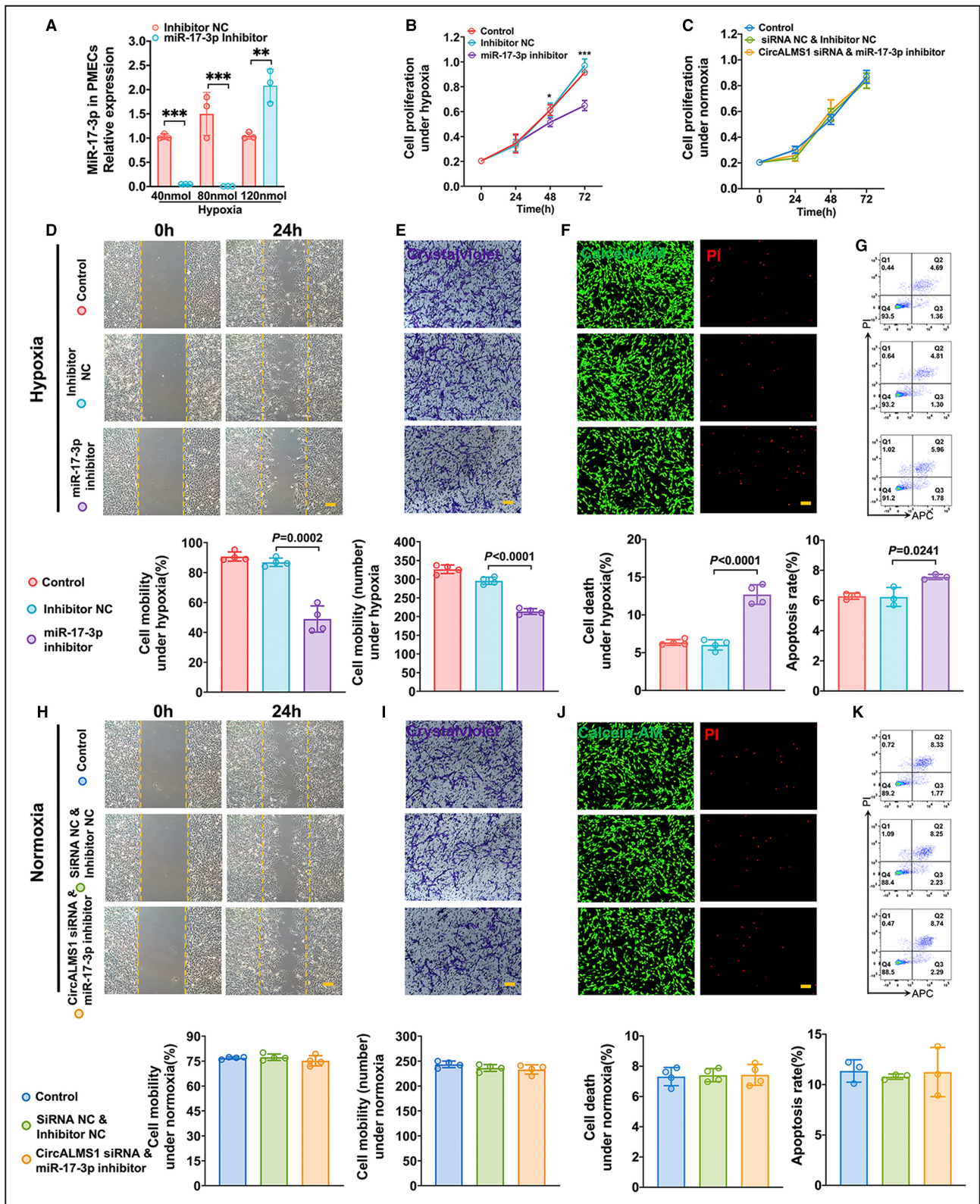
Figure 6. **MiR-17-3p inhibitor suppresses the proliferation and migration and promotes apoptosis of PMECs.**
A, The silencing efficiency of miR-17-3p in hypoxic PMECs by qRT-PCR (n=3). **B** and **D** through **G**, Cell proliferation analysis, wound healing analysis, transwell analysis, AM-PI analysis, and apoptosis analysis of PMECs with miR-17-3p inhibitor under hypoxia (n=5, 4, or 3). **C** and **H** through **K**, Cell proliferation analysis, wound healing analysis, transwell analysiss, AM-PI analysis, and apoptosis analysis of PMECs with circALMS1 siRNA and miR-17-3p inhibitor under normoxia (n=5, 4, or 3). All data are presented as mean±SD. Scale bar, 100 μm. *P<0.05; **P<0.01; ***P<0.001. AM-PI indicates calcein-AM/propidium; PMECs, pulmonary microvascular endothelial cells; qRT-PCR, quantitative reverse transcription polymerase chain reaction; and siRNA, small interfering RNA.

Figure 7.   YTHDF2 is the target of miR-17-3p in PMECs.
A, Venn diagram of predicted miR-17-3p targeted mRNA (List 1: predicted target gene of miR-17-3p by TargetScan; List 2: upregulated mRNAs of PMECs treated with circALMS1 overexpression; List 3: upregulated mRNAs of PMECs treated with miR-17-3p inhibitor; List 4: downregulated mRNAs of PMECs under hypoxia). **B**, qRT-PCR was used to validate the expression of U2AF homology motif kinase 1 and YTHDF2 in hypoxic PMECs (n=8). **C**, The protein levels of YTHDF2 in hypoxic PMECs (n=3). **D** and **E**, The protein levels of YTHDF2 in circALMS1 overexpression and circALMS1 silencing PMECs (n=3). **F** and **G**, Expression of YTHDF2 in PMECs treated with miR-17a-3p mimics and inhibitors (n=3). **H** and **I**, The mRNA and protein expression of YTHDF2 in lung tissues of control, monocrotaline, monocrotaline-AAV-NC, and monocrotaline-AAV group rats (n=6). **J** and **K**, The mRNA and protein expression of YTHDF2 in lung tissues of control, SuHx, SuHx-AAV-NC, and SuHx-AAV group rats (n=6). **L**, Dual-luciferase assays were used to examine the interactions between miR-17-3p and YTHDF2 (n=3). All data are presented as mean±SD. AAV indicates adeno-associated virus; circALMS1, circular RNA Alstrom syndrome protein 1; PMECs, pulmonary microvascular endothelial cells; qRT-PCR, quantitative reverse transcription polymerase chain reaction; SuHx, sugen/hypoxia; and YTHDF2, YT521-B homology domain-containing family protein 2.

The clinical sample analysis showed that circALMS1 expressions were significantly decreased in the plasma of 69 patients with PH as compared with 69 healthy controls (Figure 1I). The baseline characteristics of the patients with PH and healthy controls are shown in Table S3. The mean follow-up duration among patients with PH was 81.7±60.5 months. No patient was lost to follow-up. Next, we constructed the ROC curve to assess the predictive capability of circALMS1. The area under the ROC curve for patients with PH and nonsurvivors with PH was 0.756 and 0.715, respectively (Figure 1J), indicating that circALMS1 may be a promising diagnostic and prognostic indicator for PH. Based on the ROC curve analysis, patients with PH with lower circALMS1 levels in the plasma had poor outcomes (Figure 1K).

CircALMS1 Alleviates the Progression of Monocrotaline-PH and SuHx-PH in Rats

The above-mentioned results showed that circALMS1 was significantly decreased in hypoxic PMECs and plasma of patients with PH. To evaluate whether upregulated circALMS1 can alleviate the progression of monocrotaline-PH, an AAV vector based on circALMS1 (AAV-circALMS1) was delivered into rats by a transtracheal injection, followed by a subcutaneous injection of monocrotaline 14 days later (Figure 2A). Green fluorescent protein signals were observed in the pulmonary arterial intima of monocrotaline-AAV-NC and monocrotaline-AAV rats (Figure 2B). The circALMS1 expression was remarkably downregulated in the lung tissue of monocrotaline rats compared with control groups, while AAV-circALMS1 treatment upregulated circALMS1 expression in the lung tissue of monocrotaline-AAV rats (Figure 2C). The RVSP and Fulton index of rats were increased after monocrotaline treatments, whereas the AAV-circALMS1 treatments improved the RVSP and Fulton index in rats with monocrotaline-PH (Figure 2D through 2F). Echocardiography analysis showed that AAV-circALMS1 significantly attenuated right ventricular end diastolic diameter and extended the pulmonary artery acceleration time (Figure 2G and 2H). Unsurprisingly, AAV-circALMS1 remarkably attenuated the number of fully muscularized

vessels, wall thickness, collagen fiber accumulation, and thickness of the intima in rats with monocrotaline-PH (Figure 2I through 2L).

Additionally, we constructed SuHx-PH models to evaluate whether upregulated circALMS1 can alleviate the progression of SuHx-PH. The results also showed that circALMS1 alleviates the progression of SuHx-PH in rats (Figure 3).

CircALMS1 Suppresses Proliferation and Migration and Promotes Apoptosis of PMECs

To further investigate the potential impact of circALMS1 on PMECs, a vector of circALMS1 overexpression was constructed to carry out a series of cell experiments. The circALMS1 overexpression could increase its expression level by ≈4 or 5 times in hypoxic PMECs (Figure 4A). The circALMS1 upregulation could significantly inhibit cell proliferation and migration (Figure 4B, 4E, and 4F) and promote cell death of PMECs under hypoxia (Figure 4G). Further detection by flow cytometry suggested that circALMS1 could promote apoptosis of PMECs under hypoxia (Figure 4H).

To confirm the above-mentioned results, siRNA of circALMS1 was designed. Successful knockdown of circALMS1 under hypoxia was confirmed by qRT-PCR (Figure 4C). Downregulated circALMS1 significantly increased PMEC proliferation and migration (Figure 4D, 4I, and 4J) and decreased apoptosis (Figure 4K and 4L) under hypoxia.

Additionally, circALMS1 overexpression inhibited proliferation and migration and promoted apoptosis of PMECs under normoxic conditions (Figure S1). Downregulation of circALMS1 significantly increased PMEC proliferation and migration, decreased apoptosis, and promoted angiogenesis of PMECs under normoxia (Figure S2).

CircALMS1 Acts as an Efficient miRNA Sponge for miR-17-3p

To identify how circALMS1 affects proliferation, migration, and apoptosis of PMECs, we further investigated the downstream targets of circALMS1 in PMECs. As
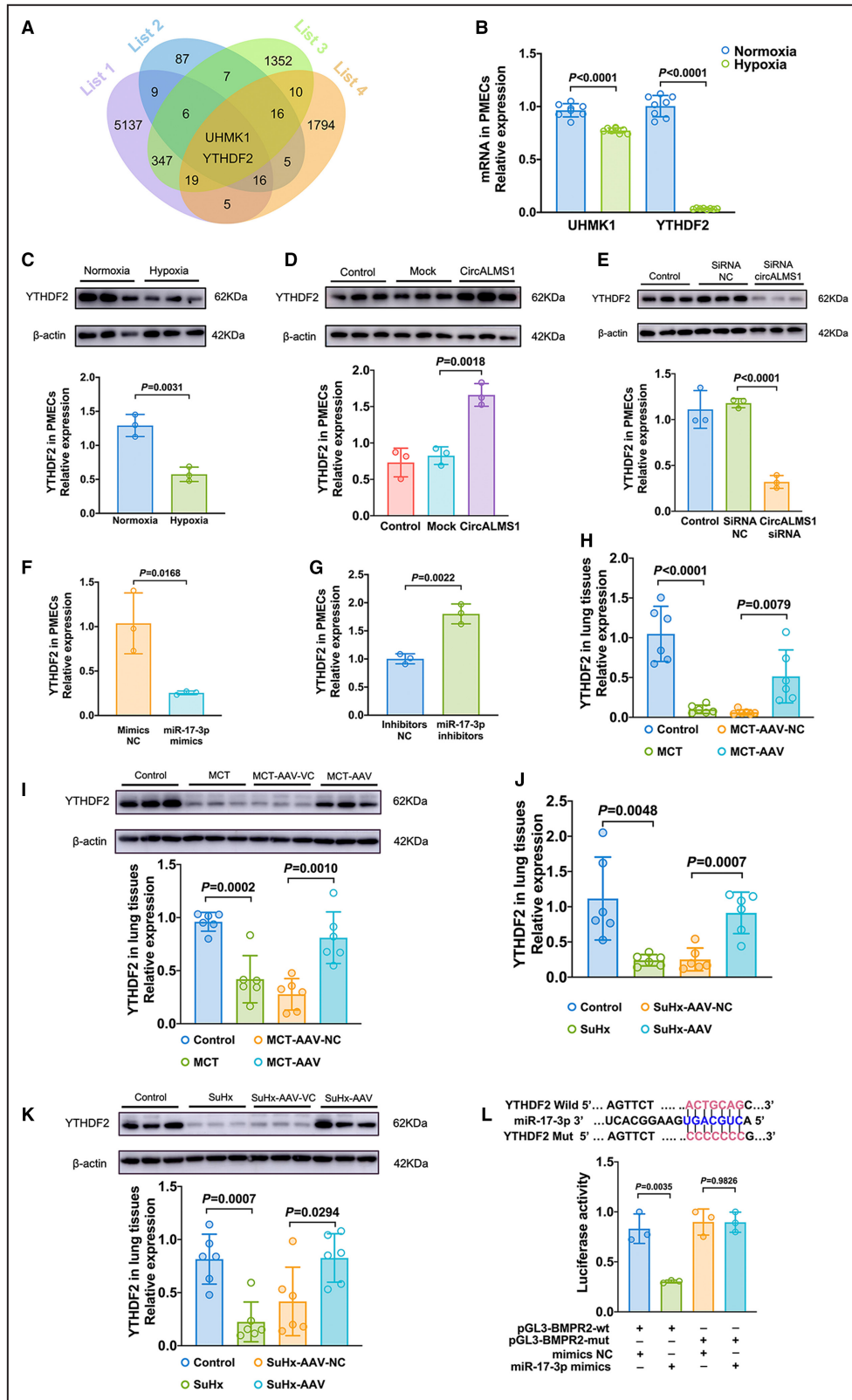
circALMS1 is mainly expressed in the cytoplasm of PMECs (Figure 1H), we considered that circALMS1 might function as an miRNA sponge.[9,21] Based on the prediction using the circAtlas, miRanda, and RNAhybrid databases, several miRNAs, including miR-337-3p, miR-17-3p, miR-518a-5p, and miR-938, might

directly interact with circALMS1. Then, those miRNAs were chosen to confirm in the following investigation. The results showed that miR-17-3p expression was significantly increased in hypoxic PMECs; however, it was significantly decreased in PMECs treated with circALMS1 overexpression (Figure 5A and 5B).

The potential binding sites between circALMS1 and miR-17-3p are shown in Figure 5C, and the predicted secondary structure for the potienal binding sites between circALMS1 and miR-17-3p is shown in Figure 5D. The dual luciferase assay results confirmed that miR-17-3p inhibited the luciferase activity of the circALMS1-WT construct but not the circALMS1-MUT construct (Figure 5C). The FISH assay also showed that circALMS1 and miR-17-3p colocalizations were observed in the cytoplasm of PMECs (Figure 5E).

MiR-17-3p Inhibitor Suppresses the Proliferation and Migration and Promotes Apoptosis of PMECs

To evaluate the effects of miR-17-3p on proliferation, migration, and apoptosis, the miR-17-3p inhibitor was used to conduct the following experiments. The miR-17-3p expression was significantly downregulated in the miR-17-3p inhibitor groups (40 and 80 nmol) as compared with the NC group (Figure 6A). Furthermore, the results showed that miR-17-3p downregulation inhibited proliferation and migration of and promoted apoptosis of PMECs under hypoxia (Figure 6B and 6D through 6G).

The above results can also be shown in normoxic PMECs with miR-17-3p inhibitor (Figure S3). Moreover, we observed cellular proliferation, migration, and apoptosis of PMECs cotransfected with miR-17-3p inhibitor and circALMS1 siRNA. Unsurprisingly, the inhibited miR-17-3p expression can significantly reverse the proliferation, migration, and apoptosis of PMECs with circALMS1 siRNA treatment (Figure 6C and 6H through 6K).

YTHDF2 Is the Target of miR-17-3p in PMECs

TargetScan was used to predict the potential target gene of miR-17-3p. Concurrently, we performed RNA sequencing to select upregulated mRNAs of PMECs

treated with circALMS1 overexpression, upregulated mRNAs of PMECs treated with a miR-17-3p inhibitor, and downregulated mRNAs of PMECs under hypoxia. After overlapping these 4 data, 2 mRNAs were selected as potential miR-17-3p targets, including U2AF homology motif kinase 1 (UHMK1) and YTHDF2 (Figure 7A). Then, YTHDF2 expression was confirmed to be more significantly downregulated in PMECs under hypoxic conditions (Figure 7B). Furthermore, the protein level of YTHDF2 was also decreased in hypoxic PMECs (Figure 7C). The protein levels of YTHDF2 were upregulated in PMECs with circALMS1 overexpression, whereas, in PMECs with circALMS1 silencing, these were downregulated (Figure 7D and 7E). The YTHDF2 expression was negatively regulated by miR-17-3p (Figure 7F and 7G). The expression of YTHDF2 was also downregulated in the lung tissues of monocrotaline-PH and SuHx-PH rats, but it was significantly upregulated in the monocrotaline-AAV and SuHx-AAV lung tissues (Figure 7H through 7K). The dual luciferase assay demonstrated that cotransfection of wild YTHDF2-3' UTR reporter and miR-17-3p mimics significantly reduced the luciferase activity in PMECs (Figure 7L).

## Silencing YTHDF2 Facilitates Proliferation and Migration and Decreases Apoptosis of PMECs

To evaluate the effects of YTHDF2 on proliferation, migration, and apoptosis, its siRNA was designed to conduct the following experiments. After verifying the knockdown efficiency of siRNA YTHDF2 in PMECs (Figure 8A), the downregulation of YTHDF2 was found to promote the proliferation and migration of PMECs and reduce apoptosis of PMECs under normoxia (Figure 8B and 8D through 8G). However, cotransfection of miR-17-3p inhibitor and siRNA YTHDF2 could reverse the effects caused by transfection of siRNA YTHDF2 in normoxic PMECs (Figure 8C and 8H through 8K), indicating that miR-17-3p affected the roles of YTHDF2 in PMECs.

The Effect of YTHDF2 on circALMS1

YTHDF2 is an m6A reader protein and contributes to the degradation of m6A-modified RNA.[22,23] M6A

Figure 8.   Silencing YTHDF2 facilitates proliferation and migration and decreases apoptosis of PMECs.
A, The silencing efficiency of YTHDF2 in normoxic PMECs by qRT-PCR (n=3). **B** and **D** through **G**, Cell proliferation analysis, wound healing analysis, transwell analysis, AM-PI analysis, and apoptosis analysis of PMECs with siRNA YTHDF2 under normoxia (n=5, 4, or 3). **C** and **H** through **K**, Cell proliferation analysis, wound healing analysis, transwell analysis, AM-PI analysis, and apoptosis analysis of PMECs with miR-17-3p inhibitor and siRNA YTHDF2 under normoxia (n=5, 4, or 3). **L**, meRIP analysis indicating that no m6A methylation occurred in circALMS1 (n=5). **M**, The protein level of YTHDF2 in PMECs-treated PMECs (n=3). **N**, Expression of circALMS1 in PMECs treated with siRNA YTHDF2 (n=3). **O**, RIP-qPCR assay was used to examine the direct interaction between YTHDF2 and circALMS1 (n=5). All data are presented as mean±SD. Scale bar, 100 μm. *P<0.05; **P<0.01; ***P<0.001. AM-PI indicates calcein-AM/propidium; IgG, immunoglobulin G; m6A, N(6)-methyladenosine; meRIP, methylated RNA immunoprecipitation; RIP, RNA immunoprecipitation; PMECs, pulmonary microvascular endothelial cells; qRT-PCR, quantitative reverse transcription polymerase chain reaction; siRNA, small interfering RNA; and YTHDF2, YT521-B homology domain-containing family protein 2.
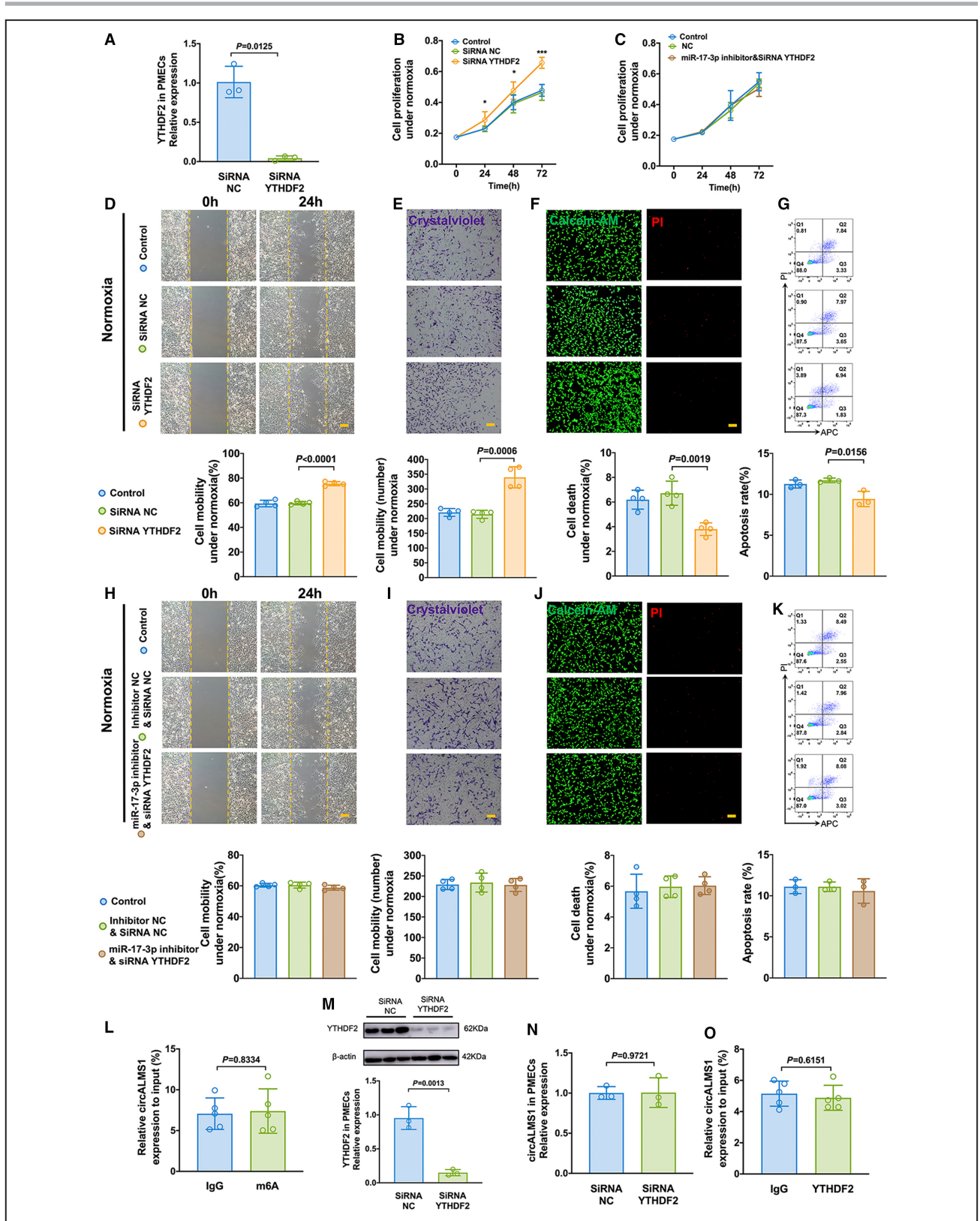
modification could exert significant roles in the metabolism of circRNAs.[24] In addition, m6A methylation predominantly occurs at the RRACH sequence (R=A or G; H=A, C, or U).[25] We found a high confident m6A site and motif (AGACA) in circALMS1 by using CircPrimer 2.0.[26] However, meRIP analysis showed that no m6A

methylation occurred in circALMS1, which was inconsistent with the prediction (Figure 8L). To further observe whether YTHDF2 could degrade cirALMS1, the siRNA of YTHDF2 was designed and its effect on cirALMS1 was observed. PMECs treated with siRNA YTHDF2 also inhibited the expression of YTHDF2 at the protein level (Figure 8M). However, the downregulation of YTHDF2 did not interfere with circALMS1 expression in PMECs (Figure 8N). Further RNA immunoprecipitation analysis indicated that there was no direct binding interaction between YTHDF2 and circALMS1 (Figure 8O).

DISCUSSION

In the present study, we identified circALMS1 to be downregulated in hypoxic PMECs and plasma of patients with PH. Upregulated circALMS1 could alleviate the pulmonary arterial remodeling and cardiac dysfunction in monocrotaline-PH and SuHx-PH rats. We further validated that lower circALMS1 expression

promoted proliferation, migration, and reduced apoptosis of PMECs. Mechanically, circALMS1 worked as an miR-17-3p sponge to regulate YTHDF2 expression, promoting proliferation, migration, and reducing apoptosis of PMECs under risk factors (Figure 9).

Recently, there have been a great number of studies on the functions of circRNAs in PH.[27,28] Our previous studies indicated that circGSAP (circular γ-secretase activating protein) was less expressed in peripheral blood mononuclear cells of patients with IPAH and the plasma of patients with IPAH and PH with chronic obstructive pulmonary disease, and circGSAP could be an emerging biomarker of the diagnosis and prognosis of IPAH and PH with chronic obstructive pulmonary disease.[19,20,29] In the present study, we focused on another circRNA, namely, circALMS1, and found that circALMS1 was downregulated in the plasma of patients with PH and hypoxic PMECs. Although these 2 circRNAs were all downregulated in the plasma of patients with
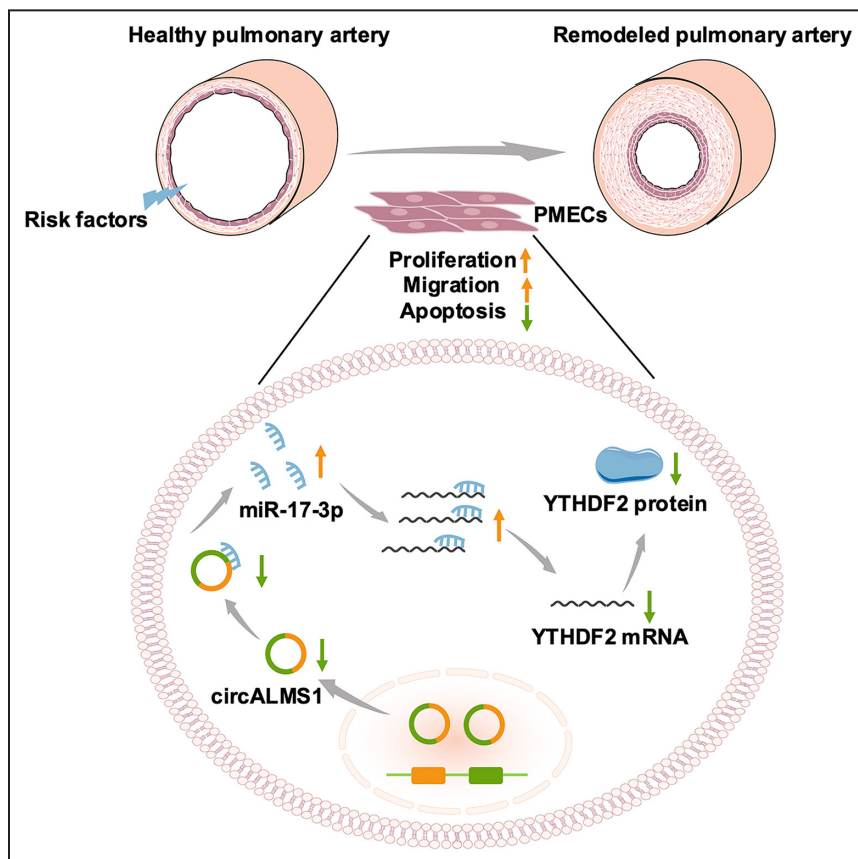
Figure 9. A schematic diagram indicates that circALMS1 worked as an miR-17-3p sponge to regulate the expression of YTHDF2, promoting proliferation and migration and reducing apoptosis of PMECs under risk factors.
CircALMS1 indicates circular RNA Alstrom syndrome protein 1; PMECs, pulmonary microvascular endothelial cells; and YTHDF2, YT521-B homology domain-containing family protein 2.

PH, they were screened from different sequencing analyses. CircGSAP was screened from peripheral blood mononuclear cells of patients with IPAH and healthy controls, whereas circALMS1 was a differentially expressed circRNA between normoxic and hypoxic PMECs, indicating that circALMS1 might be more specific to the inner membrane or ECs under hypoxia. Furthermore, we then used overexpression plasmid and siRNA-mediated the up- and downexpression of circALMS1 to examine its effect on PMEC proliferation, migration, and apoptosis; we found that downregulated circALMS1 is a critical process in PMECs dysfunction under hypoxia, suggesting that circALMS1 may be a protective factor for PMECs under physiological conditions.

CircRNAs play significant roles in physiological processes via 3 main pathways,[21] among which the sponge mechanism was the widely studied function of circRNAs in PH.[16,17,19,20] Our previous studies suggested that lower circGSAP expression increased cell proliferation and migration and reduced cell death through the miR-27a-3p/bone morphogenetic protein receptor type II and miR-942-5p/mothers against decapentaplegic homolog 4 axis in PMECs.[19,20] However, studies on the function of circRNAs in ECs are insufficient. Because circALMS1 expression is located in the cytoplasm, we also focused on the sponge mechanism of circALMS1 in this study. Our data indicated that circALMS1 acted as an miR-17-3p sponge and promoted proliferation and migration and reduced apoptosis of PMECs. Additionally, we also investigated the function of circAMSM1 on angiogenesis and found that knocking the expression of circALMS1 promoted angiogenesis. However, the effect of circALMS1 on angiogenesis was not as effective as compared with its other functions, such as cell proliferation, migration, and apoptosis. Therefore, we primarily focused on investigating the role of circAMSL1-targeted miRNA and mRNA in regulating proliferation, migration, and apoptosis of PMECs in the following study.

MiR-17-3p was widely studied in various diseases.[30–32] It was reported that miR-17-3p contributed to exercise-induced cardiac growth and protected against myocardial ischemia–reperfusion injury.[30] However, research on the miR-17-3p expression in PH is lacking. Our results indicated that miR-17-3p might be involved in PH pathogenesis by regulating the function of PMECs. One previous study explored the role of miR-17-3p in endothelial inflammation; miR-17-3p was found to suppress nuclear factor-κ-light-chain enhancer of activated B cell–mediated endothelial inflammation by targeting nuclear factor-κ-light-chain enhancer of activated B cell–inducing kinase and IκB kinase β–binding protein.[32] However, future studies should explore whether miR-17-3p is a proinflammatory factor involved in the process of PMEC damage under pathological conditions of PH.

Our study indicated that miR-17-3p inhibited YTHDF2 expression. YTHDF2 is an m6A reader and is associated with increased degradation of target transcripts.[33] Particularly, endoribonucleolytic cleavage of the m6A-modified circRNAs by YTHDF2-HRSP12-RNase P/MRP complex has been reported.[34] For example, a previous study reported that YTHDF2-mediated m6A modification drives the degradation of circ_0003215.[22] Although we found a high confident m6A site and motif (AGACA) in circALMS1 by prediction, further meRIP analysis showed no m6A methylation occurred in circALMS1. RNA immunoprecipitation assay and qRT-PCR were shown to observe whether YTHDF2 would downregulate circALMS1. The results indicated that YTHDF2 could not capture circALMS1 and regulate the circALMS1 levels in PMECs. Therefore, while YTHDF2 is a downstream regulator of circALMS1, circALMS1 is not a downstream target for YTHDF2. Additionally, YTHDF2 was downregulated in hypoxic PMECs, silencing YTHDF2 promoted cell proliferation and migration and reduced apoptosis of PMECs, suggesting that YTHDF2 plays a role in regulating PMECs function. However, 2 studies found that hypoxia increased the expression of YTHDF2 in pulmonary arterial smooth muscle cells and alveolar macrophages,[35,36] which contradicts our results. This could be due to different cellular microenvironments. Of course, the underlying mechanism needs to be further explored.

The present study still has some limitations. First, we only identified the molecular mechanism of circALMS1 as a sponge to regulate PMEC functions. Other molecular mechanisms, such as binding RNA-binding proteins and translating into proteins, have not been studied. Second, >1 miRNA could be a circALMS1 sponge, and we only detected the function of miR-17-3p. Finally, other cells, such as the pulmonary arterial smooth muscle cells, pericytes, fibroblasts, and macrophages, also play significant roles in PH; however, whether circALMS1 exists and functions in these cells remains unclear.

In conclusion, low circALMS1 levels could predict the poor outcomes of patients with PH, which may be due to the fact that downregulated circALMS1 promoted proliferation and migration and reduced apoptosis of PMECs via the miR-17-3p/YTHDF2 axis. Overexpression of circALMS1 could alleviate the progression in monocrotaline-PH and SuHx-PH rats. Our study provided relevant and novel data to understand the underlying mechanisms of pulmonary vascular remodeling, which could lead to the development of new therapeutic targets for PH.

ARTICLE INFORMATION

Affiliations

Department of Cardio-Pulmonary Circulation, Shanghai Pulmonary Hospital, School of Medicine, Tongji University, Shanghai, China (X.H., S.W., H.Z., Y.W., J.F., Y.H., W.W., J.L., J.L., S.G., Q.Z., L.W., R.J., P.Y.); Department of Respiratory and Critical Care Medicine, Shandong Provincial Hospital Affiliated to Shandong First Medical University, Jinan, China (Y.S.); Institute of Bismuth Science, University of Shanghai for Science and Technology, Shanghai, China (H.Z.); Department of Geriatrics, Shanghai Institute of Geriatrics, Huadong Hospital, Fudan University, Shanghai, China (Y.W.); Institute of Health Science and Engineering, University of Shanghai Science and Technology, Shanghai, China (J.F.); and Department of Thoracic Surgery, Shanghai Pulmonary Hospital, School of Medicine, Tongji University, Shanghai, China (X.S.).

Sources of Funding

Disclosures

None.

Supplemental Material

Tables S1–S3
Figures S1–S3

REFERENCES

1. Cober ND, VandenBroek MM, Ormiston ML, Stewart DJ. Evolving concepts in endothelial pathobiology of pulmonary arterial hypertension. *Hypertension*. 2022;79:1580–1590. doi: 10.1161/HYPERTENSIONAHA.122.18261

2. Aldred MA, Morrell NW, Guignabert C. New mutations and pathogenesis of pulmonary hypertension: progress and puzzles in disease pathogenesis. *Circ Res*. 2022;130:1365–1381. doi: 10.1161/CIRCRESAHA.122.320084

3. Adir Y, Humbert M, Chaouat A. Sleep-related breathing disorders and pulmonary hypertension. *Eur Respir J*. 2021;57:2002258. doi: 10.1183/13993003.02258-2020

4. Simonneau G, Montani D, Celermajer DS, Denton CP, Gatzoulis MA, Krowka M, Williams PG, Souza R. Haemodynamic definitions and updated clinical classification of pulmonary hypertension. *Eur Respir J*. 2019;53:1801913. doi: 10.1183/13993003.01913-2018

5. Wang Q, Tian J, Li X, Liu X, Zheng T, Zhao Y, Li X, Zhong H, Liu D, Zhang W, et al. Upregulation of endothelial DKK1 (Dickkopf 1) promotes the development of pulmonary hypertension through the Sp1 (specificity protein 1)/SHMT2 (serine Hydroxymethyltransferase 2) pathway. *Hypertension (Dallas, Tex: 1979)*. 2022;79:960–973. doi: 10.1161/HYPERTENSIONAHA.121.18672

6. Humbert M, Guignabert C, Bonnet S, Dorfmuller P, Klinger JR, Nicolls MR, Olschewski AJ, Pullamsetti SS, Schermuly RT, Stenmark KR, et al. Pathology and pathobiology of pulmonary hypertension: state of the art and research perspectives. *Eur Respir J*. 2019;53:1801887. doi: 10.1183/13993003.01887-2018

7. MacIver DH, Adeniran I, MacIver IR, Revell A, Zhang H. Physiological mechanisms of pulmonary hypertension. *Am Heart J*. 2016;180:1–11. doi: 10.1016/j.ahj.2016.07.003

8. Waxman A, Restrepo-Jaramillo R, Thenappan T, Ravichandran A, Engel P, Bajwa A, Allen R, Feldman J, Argula R, Smith P, et al. Inhaled Treprostinil in pulmonary hypertension due to interstitial lung disease. *N Engl J Med*. 2021;384:325–334. doi: 10.1056/NEJMoa2008470

9. Hansen TB, Jensen TI, Clausen BH, Bramsen JB, Finsen B, Damgaard CK, Kjems J. Natural RNA circles function as efficient microRNA sponges. *Nature*. 2013;495:384–388. doi: 10.1038/nature11993

10. Wilusz JE, Sharp PA. Molecular biology. A circuitous route to noncoding RNA. *Science (New York, NY)*. 2013;340:440–441. doi: 10.1126/science.1238522

11. Lyu D, Huang S. The emerging role and clinical implication of human exonic circular RNA. *RNA Biol*. 2017;14:1000–1006. doi: 10.1080/15476286.2016.1227904

12. Yang H, Li X, Meng Q, Sun H, Wu S, Hu W, Liu G, Li X, Yang Y, Chen R. CircPTK2 (hsa_circ_0005273) as a novel therapeutic target for metastatic colorectal cancer. *Mol Cancer*. 2020;19:13. doi: 10.1186/s12943-020-1139-3

13. Szabo L, Salzman J. Detecting circular RNAs: bioinformatic and experimental challenges. *Nat Rev Genet*. 2016;17:679–692. doi: 10.1038/nrg.2016.114

14. Vo JN, Cieslik M, Zhang Y, Shukla S, Xiao L, Zhang Y, Wu YM, Dhanasekaran SM, Engelke CG, Cao X, et al. The landscape of circular RNA in cancer. *Cell*. 2019;176:869–881. doi: 10.1016/j.cell.2018.12.021.e13

15. Ma C, Gu R, Wang X, He S, Bai J, Zhang L, Zhang J, Li Q, Qu L, Xin W, et al. circRNA CDR1as promotes pulmonary artery smooth muscle cell calcification by upregulating CAMK2D and CNN3 via sponging miR-7-5p. *Molecular Therapy Nucleic Acids*. 2020;22:530–541. doi: 10.1016/j.omtn.2020.09.018

16. Zhang J, Li Y, Qi J, Yu X, Ren H, Zhao X, Xin W, He S, Zheng X, Ma C, et al. Circ-calm4 serves as an miR-337-3p sponge to regulate Myo10 (myosin 10) and promote pulmonary artery smooth muscle proliferation. *Hypertension (Dallas, Tex: 1979)*. 2020;75:668–679. doi: 10.1161/HYPERTENSIONAHA.119.13715

17. Jiang Y, Liu H, Yu H, Zhou Y, Zhang J, Xin W, Li Y, He S, Ma C, Zheng X, et al. Circular RNA Calm4 regulates hypoxia-induced pulmonary arterial smooth muscle cells Pyroptosis via the circ-Calm4/miR-124-3p/PDCD6 Axis. *Arterioscler Thromb Vasc Biol*. 2021;41:1675–1693. doi: 10.1161/ATVBAHA.120.315525

18. Galie N, Humbert M, Vachiery JL, Gibbs S, Lang I, Torbicki A, Simonneau G, Peacock A, Vonk Noordegraaf A, Beghetti M, et al. 2015 ESC/ERS guidelines for the diagnosis and treatment of pulmonary hypertension: the joint task force for the diagnosis and treatment of pulmonary hypertension of the European Society of Cardiology (ESC) and the European Respiratory Society (ERS): endorsed by: Association for European Paediatric and Congenital Cardiology (AEPC), International Society for Heart and Lung Transplantation (ISHLT). *Eur Heart J*. 2016;37:67–119. doi: 10.1093/eurheartj/ehv317

19. Sun Y, Jiang R, Hu X, Gong S, Wang L, Wu W, Li J, Kang X, Xia S, Liu J, et al. CircGSAP alleviates pulmonary microvascular endothelial cells dysfunction in pulmonary hypertension via regulating miR-27a-3p/BMPR2 axis. *Respir Res*. 2022;23:322. doi: 10.1186/s12931-022-02248-7

20. Sun Y, Wu W, Zhao Q, Jiang R, Li J, Wang L, Xia S, Liu M, Gong S, Liu J, et al. CircGSAP regulates the cell cycle of pulmonary microvascular endothelial cells via the miR-942-5p sponge in pulmonary hypertension. *Front Cell Dev Biol*. 2022;10:967708. doi: 10.3389/fcell.2022.967708

21. Kristensen LS, Andersen MS, Stagsted LVW, Ebbesen KK, Hansen TB, Kjems J. The biogenesis, biology and characterization of circular RNAs. *Nat Rev Genet*. 2019;20:675–691. doi: 10.1038/s41576-019-0158-7

22. Chen B, Hong Y, Gui R, Zheng H, Tian S, Zhai X, Xie X, Chen Q, Qian Q, Ren X, et al. N6-methyladenosine modification of circ_0003215 suppresses the pentose phosphate pathway and malignancy of colorectal cancer through the miR-663b/DLG4/G6PD axis. *Cell Death Dis*. 2022;13:804. doi: 10.1038/s41419-022-05245-2

23. Zaccara S, Jaffrey SR. A unified model for the function of YTHDF proteins in regulating m(6)A-modified mRNA. *Cell*. 2020;181:1582–1595. doi: 10.1016/j.cell.2020.05.012.e18

24. Zhang L, Hou C, Chen C, Guo Y, Yuan W, Yin D, Liu J, Sun Z. The role of N(6)-methyladenosine (m(6)a) modification in the regulation of circRNAs. *Mol Cancer*. 2020;19:105. doi: 10.1186/s12943-020-01224-3

25. Ping XL, Sun BF, Wang L, Xiao W, Yang X, Wang WJ, Adhikari S, Shi Y, Lv Y, Chen YS, et al. Mammalian WTAP is a regulatory subunit of the RNA N6-methyladenosine methyltransferase. *Cell Res*. 2014;24:177–189. doi: 10.1038/cr.2014.3

26. Zhong S, Feng J. CircPrimer 2.0: a software for annotating circRNAs and predicting translation potential of circRNAs. *BMC Bioinformatics*. 2022;23:215. doi: 10.1186/s12859-022-04705-y

27. Ali MK, Schimmel K, Zhao L, Chen CK, Dua K, Nicolls MR, Spiekerkoetter E. The role of circular RNAs in pulmonary hypertension. *Eur Respir J*. 2022;60:2200012. doi: 10.1183/13993003.00012-2022

28. Wang Q, Sun Y, Zhao Q, Wu W, Wang L, Miao Y, Yuan P. Circular RNAs in pulmonary hypertension: emerging biological concepts and potential mechanism. *Animal Model Exp Med*. 2022;5:38–47. doi: 10.1002/ame2.12208

29. Yuan P, Wu WH, Gong SG, Jiang R, Zhao QH, Pudasaini B, Sun YY, Li JL, Liu JM, Wang L. Impact of circGSAP in peripheral blood mononuclear cells on idiopathic pulmonary arterial hypertension. *Am J Respir Crit Care Med*. 2021;203:1579–1583. doi: 10.1164/rccm.202005-2052LE

30. Shi J, Bei Y, Kong X, Liu X, Lei Z, Xu T, Wang H, Xuan Q, Chen P, Xu J, et al. miR-17-3p contributes to exercise-induced cardiac growth and protects against myocardial ischemia-reperfusion injury. *Theranostics*. 2017;7:664–676. doi: 10.7150/thno.15162

31. Xiang P, Yeung YT, Wang J, Wu Q, Du R, Huang C, Jia X, Gao Y, Zhi Y, Guo F, et al. miR-17-3p promotes the proliferation of multiple myeloma cells by downregulating P21 expression through LMLN inhibition. *Int J Cancer*. 2021;148:3071–3085. doi: 10.1002/ijc.33528

32. Ji J, Fu J. MiR-17-3p facilitates aggressive cell phenotypes in colon cancer by targeting PLCD1 through affecting KIF14. *Appl Biochem Biotechnol*. 2022;195:1723–1735. doi: 10.1007/s12010-022-04218-7

33. Wang X, Zhao BS, Roundtree IA, Lu Z, Han D, Ma H, Weng X, Chen K, Shi H, He C. N(6)-methyladenosine modulates messenger RNA translation efficiency. *Cell*. 2015;161:1388–1399. doi: 10.1016/j.cell.2015.05.014

34. Park OH, Ha H, Lee Y, Boo SH, Kwon DH, Song HK, Kim YK. Endoribonucleolytic cleavage of m(6)A-containing RNAs by RNase P/MRP complex. *Mol Cell*. 2019;74:494–507. doi: 10.1016/j.molcel.2019.02.034.e8

35. Hu L, Yu Y, Shen Y, Huang H, Lin D, Wang K, Yu Y, Li K, Cao Y, Wang Q, et al. Ythdf2 promotes pulmonary hypertension by suppressing Hmox1-dependent anti-inflammatory and antioxidant function in alveolar macrophages. *Redox Biol*. 2023;61:102638. doi: 10.1016/j.redox.2023.102638

36. Qin Y, Qiao Y, Li L, Luo E, Wang D, Yao Y, Tang C, Yan G. The m(6)a methyltransferase METTL3 promotes hypoxic pulmonary arterial hypertension. *Life Sci*. 2021;274:119366. doi: 10.1016/j.lfs.2021.119366